

## Real-time detection of linear and angular displacements with a modified DVD optical head

This article has been downloaded from IOPscience. Please scroll down to see the full text article.

2008 Nanotechnology 19 115501

(<http://iopscience.iop.org/0957-4484/19/11/115501>)

View [the table of contents for this issue](#), or go to the [journal homepage](#) for more

### Download details:

IP Address: 140.109.103.227

The article was downloaded on 25/05/2011 at 06:43

Please note that [terms and conditions apply](#).

# Real-time detection of linear and angular displacements with a modified DVD optical head

En-Te Hwu<sup>1</sup>, Shao-Kang Hung<sup>1</sup>, Chih-Wen Yang<sup>1</sup>,  
Kuang-Yuh Huang<sup>2</sup> and Ing-Shouh Hwang<sup>1</sup>

<sup>1</sup> Institute of Physics, Academia Sinica, Nankang, Taipei, Taiwan

<sup>2</sup> Department of Mechanical Engineering, National Taiwan University, Taipei, Taiwan

E-mail: [ishwang@phys.sinica.edu.tw](mailto:ishwang@phys.sinica.edu.tw)

Received 5 December 2007

Published 18 February 2008

Online at [stacks.iop.org/Nano/19/115501](http://stacks.iop.org/Nano/19/115501)

## Abstract

Here we demonstrate that an astigmatic detection system (ADS), constructed with a modified digital-versatile-disk (DVD) optical head, can achieve real-time measurement of a linear displacement and two-dimensional (2D) tilt angles with a high sensitivity. An atomic force microscope (AFM), using our detection system to sense the deflection of microfabricated cantilevers, can resolve single atomic steps on graphite surfaces with a noise level less than 0.04 nm in topographic images. This astigmatic detection system can even detect mechanical resonances due to thermal vibrations of microfabricated cantilevers. The high sensitivity, small detecting size and high bandwidth of this detection system is suitable for dynamic characterization of elements in micromachined components. Further optimization of the system will promise many other applications in diverse technological fields.

(Some figures in this article are in colour only in the electronic version)

## 1. Introduction

Atomic force microscopy (AFM) and its related scanning probe microscopies (SPMs) have been widely used to probe various surface properties at the nanometer or atomic level [1, 2]. In AFM, usually a microfabricated cantilever is used to sense the weak interactions between the tip and the surface. The weak forces can induce a small deflection or changes in the mechanical resonances of the cantilever. In recent years, there has been spectacular development in the chemical/biological sensors based on static deformations or dynamic motions of suspended elements in micro- and nanoelectromechanical systems (MEMSs and NEMSs) [3–7]. In engineering and nano/bio-technological fields, there have been a number of MEMS sensors and actuators developed for various applications. It is often essential to detect the deformations or resonant motions of suspended elements such as single-clamped cantilevers, double-clamped bridges and membranes. The mechanical movements of these elements vary from position to position. The motions at a local position involve the linear displacement in the direction normal to the

plane of the element (the vertical displacement) and/or two-dimensional angular tilt relative to the normal direction of the plane. At certain positions of the elements, the vertical displacement is more significant than the angular changes; but at some other positions, the angular changes are more significant than the vertical displacement. For example, in the bending mechanical resonances of these suspended elements, the nodes exhibit zero vertical displacement and maximum oscillation amplitude in the slope (angular) changes; the anti-nodes exhibit zero slope (angular) changes and maximum oscillation amplitude in the vertical displacement. Also, the torsional resonances of a cantilever involve only angular changes around the main axis of the cantilever but with no height variation on the axis. Therefore, to fully characterize these motions, it is important to access the vertical displacement and two-dimensional (2D) tilt angles simultaneously with a high enough bandwidth at any arbitrary position of the suspended elements.

Current detection methods measure either the one-dimensional (1D) vertical displacement (e.g. laser interferometry [8, 9], capacitance measurement [10]) or the 1D/2D an-

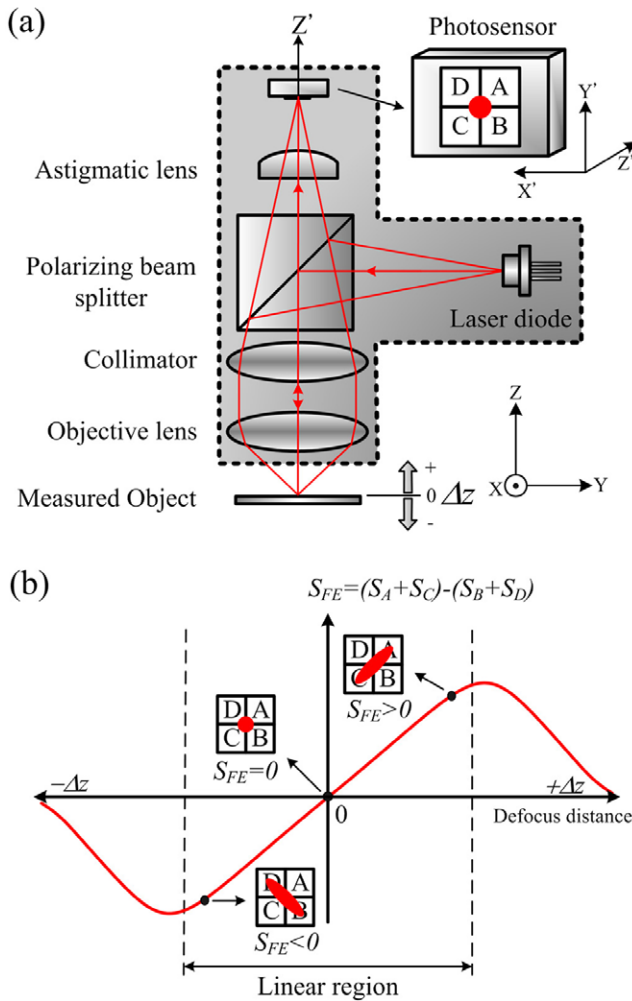


**Figure 1.** (a) Schematic diagram of a typical astigmatic optical path. The  $X$ - $Y$ - $Z$  axes are defined at the position of the object surface with the  $Z$  axis as the optical axis of the laser beam. The  $X'$ - $Y'$ - $Z'$  axes are defined at the position of the photosensor. (b)  $S_{FE}$  versus defocus distance. The corresponding light spot projected on the photosensor is shown at three different defocus distances.

gular displacements (e.g. laser beam deflection method [11]), and they have been successfully adopted in AFM and MEMSs/NEMSs-based chemical/biological sensors. In this work, we demonstrate that the astigmatic detection scheme used in most compact disk (CD)/DVD read-only memory (ROM) drives [12–14] can simultaneously detect the vertical displacement and two-dimensional angular tilt at arbitrary local positions on microfabricated cantilevers with a high sensitivity and a high bandwidth.

Figure 1(a) illustrates a typical astigmatic optical path that can be found in many CD/DVD optical heads. A laser beam emitted from a laser diode is first collimated and then focused onto an object surface by an objective lens. The beam reflected from the object surface is then directed back through the lenses and, after passing through an astigmatic element [15] (such as a cylindrical lens or a tilted glass plate), impinges onto a photodetector integrated chip (PDIC). The center of the PDIC is composed of four quadrant photosensors (A, B, C, D) with a current preamplifier for each of them. The astigmatic element

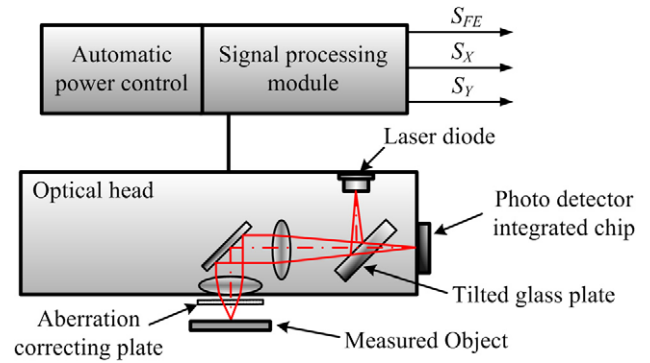


**Figure 2.** Schematic drawing of our astigmatic detection system. The tilted glass plate works as a beamsplitter for the emitted laser beam and as the astigmatic element for the reflected beam.

is a beam-shaping device. As shown in figure 1(b), when the object surface is perfectly at the focus point of the laser beam (defocus distance  $\Delta z = 0$ ), the light spot projected on the photosensors is circular; when the surface is slightly higher or lower than the focus point of the laser beam, the light spot becomes more elongated with the long axis of the spot along the AC or DB direction, respectively. The shape change of the light spot can be detected with the focus error signal ( $S_{FE}$ ), which is defined as  $(S_A + S_C) - (S_B + S_D)$ , where  $S_A \sim S_D$  are the preamplifier output voltages of photosensors A  $\sim$  D, respectively. For a circular light spot ( $\Delta z = 0$ ),  $S_{FE} = 0$ . Figure 1(b) shows the well-known S-shaped curve for the relationship of  $S_{FE}$  versus the defocus distance of the object surface. There is a linear region for the  $S_{FE}$  signal versus  $\Delta z$ , so the  $S_{FE}$  signal in this region can be used to measure the height and linear displacement of an object surface along the optical axis ( $Z$  axis). Several previous studies demonstrated that the height signal  $S_{FE}$  could measure the vertical displacement along the  $Z$  axis with a resolution of several nm or larger [16–18].

Our astigmatic detection system is based on modification of a commercial DVD optical head. It can achieve a resolution better than 0.3 nm in detection of the vertical displacement and, most importantly, it can also detect the two-dimensional angular tilt of the object surface. This system can detect small mechanical resonances due to thermal motions of microfabricated cantilevers. Since measurements of linear displacement and angular changes are essential in a variety of technologies, this detection scheme may promise many other applications, such as nanopositioning [19], accelerometers [20], alignment of small objects, 3D profilometer [21] for surface profile inspection, etc.

## 2. Experimental details

The schematic drawing of our astigmatic detection system is shown in figure 2. A slim-type CD/DVD optical head (TOP1100S from Topray Technologies Inc.) is used. The laser module of the optical head emits light at the two wavelengths of 655 and 790 nm, used for DVD and CD, respectively. Here we use only the laser beam of 655 nm, because it is visible and

the focus spot is smaller than that of the other beam. We have also removed a diffraction grating placed right behind the laser diode. The objective lens (with a numerical aperture of 0.6 and a focal length of 2.33 mm) is normally suspended by a voice-coil motor in the optical head. To achieve a good mechanical stability, the objective lens is firmly attached to the frame of the optical head with epoxy. An aberration correcting plate is inserted between the objective lens and the object surface, because the objective lens is specially designed to focus on a surface through a certain thickness of the polycarbonate film of optical disks. To detect local motions of microfabricated AFM cantilevers, the detection system is mounted on a three-axis translation stage and a rotary stage to accurately position it to focus the laser spot at a desired position over the upper surface of the cantilever and to align it with a desired orientation relative to the cantilever, respectively.

Our home-made electronics comprise an automatic power control circuitry (APC) and a signal processing module. The APC is used to drive the laser diode of the optical head and to stabilize the emitted optical power ( $\sim 0.23$  mW). The signal processing module is designed to generate the height and angular signals from the preamplifier output voltages of photosensors A–D.

Two type of AFM cantilevers are used in this work. A type of stiff cantilever (AR5-NCHR AFM tips from NANOSENSORS with a force constant of  $10\text{--}130$  N m $^{-1}$  and a resonance frequency of  $204\text{--}497$  kHz) is used for AFM topographic imaging. All other measurements use a type of soft cantilever, PPP-CONTR-50 from NANOSENSORS with the beam dimensions of  $450 \times 50 \times 2$   $\mu\text{m}^3$ . In the measurement of thermal noise spectra, the spectra of the soft cantilevers are obtained by feeding one of the height and angular signals into a high-speed 16-bit analog-to-digital converter (ADC) of a commercial AFM system (Asylum Research, MFP-3D-BIO), which is then analyzed with the IGOR Pro software. All the experiments presented here are carried out in ambient conditions with the room temperature at  $\sim 23$  °C.

### 3. Results and discussion

#### 3.1. Detection of the vertical displacement

We have measured the S-curve of our astigmatic detection system on a mirror, whose linear displacement is driven by a piezo-stack and calibrated with a commercial interferometer (SP-S120, SIOS Meßtechnik GmbH). As shown in figure 3(a), a linear region of  $\sim 6$   $\mu\text{m}$  is seen for the  $S_{FE}$  signal versus the defocus distance. In figure 3(b), the mirror is actuated by a piezo-stack with a triangular wave at a frequency of 0.5 Hz and the  $S_{FE}$  signal can detect its periodic displacement of 10 nm. The root-mean-square noise of the  $S_{FE}$  signal is measured to be 0.53 nm without any filter and 0.047 nm with a 10 kHz low-pass filter. The resolution is much better than that of previous works using CD/DVD optical heads to detect the vertical displacement [16–18, 22].

#### 3.2. Detection of two-dimensional angular displacements

We find that this astigmatic detection system can also detect the 2D tilt angles of the object surface relative to the Z axis.

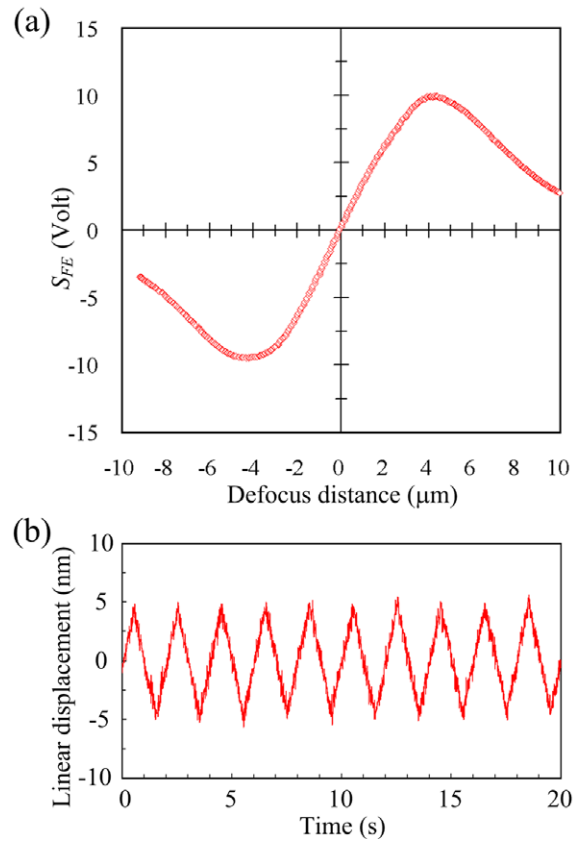


**Figure 3.** Measurement of height using the  $S_{FE}$  signal of our astigmatic detection system. (a) Measured S-curve with the defocus distance calibrated by a commercial interferometer. (b) Measurement of small movements of a mirror with the  $S_{FE}$  signal.

A schematic drawing for the tilting is illustrated in figure 4, based on our monitoring of the light spot on the quadrant photosensors. We find that rotation of the object surface around an axis perpendicular to the Z axis leads to translation of the light spot but with little shape change. If rotation of the object surface around an axis can lead to translation of the light spot along the  $X'$  axis of the photosensor, we define such an axis as the X axis. Similarly, the Y axis can be defined. Thus, it may be possible to use the angular signal  $S_X$ , where  $S_X = (S_C + S_D) - (S_A + S_B)$ , to detect the angular change for rotation around the X axis. Similarly, the angular signal  $S_Y$ , defined as  $(S_A + S_D) - (S_B + S_C)$ , may be used to detect the angular change around the Y axis.

Since tilting a surface using a rotary stage usually involves an unknown height change and that it cannot be guaranteed that the same surface spot is detected after the rotation, a special experiment as shown in figure 5(a) is designed to test whether the  $S_X$  and  $S_Y$  signals can detect pure angular changes. A microfabricated AFM cantilever is placed on a knife edge which is stationary relative to our astigmatic detection system (ADS). The base chip of the probe is moved up and down through actuation of a piezo-stack. At the position of the cantilever directly on top of the knife edge, one would expect that only angular changes of the cantilever with little vertical displacement is detected. Measurements shown in figure 5(b) do exhibit a significant change of  $\sim 400$   $\mu\text{rad}$  in the  $S_Y$  signal

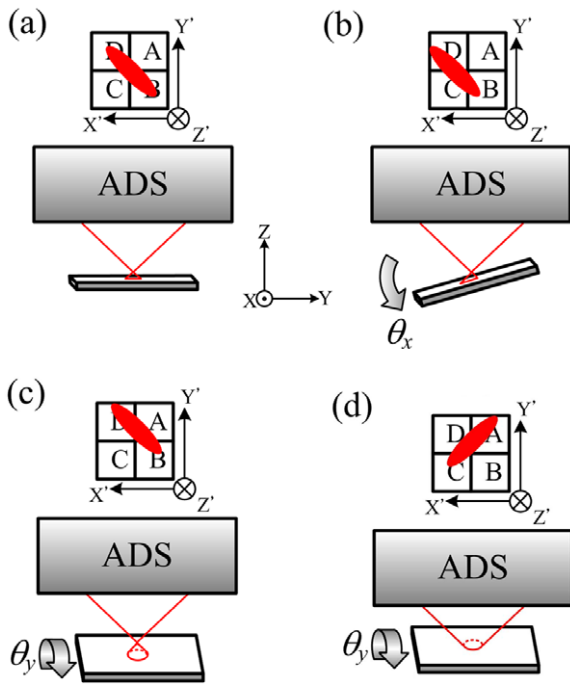


**Figure 4.** Translation of the projected light spot on the photosensor caused by tilting the object surface. ADS represents the astigmatic detection system. (a) Schematic drawing of the measurement without any tilt of the object surface, i.e. the object surface is normal to the optical axis.  $\Delta z < 0$ . (b) Schematic drawing of the measurement for rotation of the object surface around the X axis.  $\Delta z < 0$ . (c) Schematic drawing of the measurement for rotation around the Y axis.  $\Delta z < 0$ . (d) Schematic drawing for rotation around the Y axis.  $\Delta z > 0$ . For other defocus distances and other tilting orientations, similar translation of the light spot on the photosensor can be expected.

but only a very small change of  $\sim 0.6$  nm in  $S_{FE}$ , when the actuation of the base chip is 64 nm. Similar results are obtained with the  $S_{FE}$  and  $S_X$  signals when our detection system is rotated  $90^\circ$  around the Z axis. These clearly indicate that the  $S_X$  and  $S_Y$  signals can be used to measure the change in the tilt angles of a local surface spot. The root-mean-square noise of the  $S_X$  and  $S_Y$  signals is  $42 \mu\text{rad}$  without any filter and  $3.5 \mu\text{rad}$  with a 10 kHz low-pass filter.

3.3. Application of the astigmatic detection system to atomic force microscopy

A commercial AFM (Nanoscope III of Digital Instrument Inc.) is modified by replacing the beam deflection module with our astigmatic detection system. A schematic drawing of the modification is shown in figure 6. A probe clamping module (PCM) is designed to hold an AFM cantilever. The PCM is very carefully attached to the optical head, so that the focus spot of the laser beam is right on the back surface of the cantilever. The entire optical head-PCM assembly is very compact and rigid, so that it has a good mechanical stability during the AFM operation. In order to eliminate any need for realignment when the cantilever is changed, an alignment chip from NANOSENSORS is used in our PCM. The bending motions of the cantilever can be detected with either  $S_{FE}$  or  $S_Y$ .

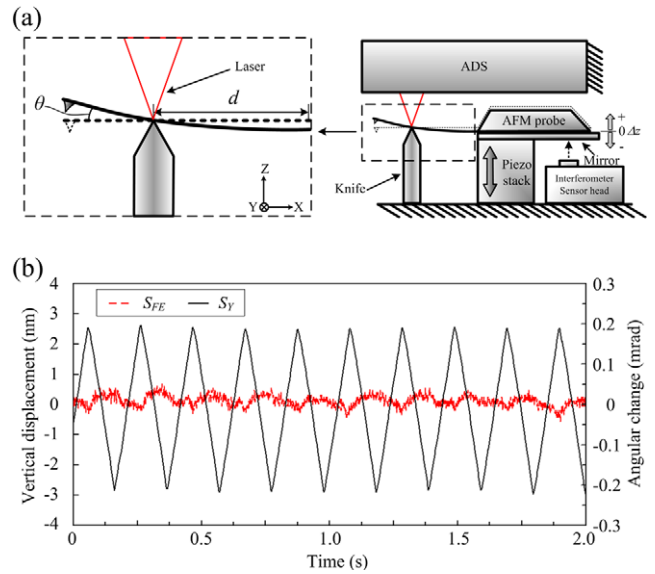


**Figure 5.** (a) Schematic drawing of the measurement. The piezo-stack is driven with a triangular wave at a frequency of 5 Hz. The peak-to-peak displacement of the base chip is 64 nm, as determined with a commercial interferometer (SP-S120, SIOS Meßtechnik GmbH).  $d = 230 \mu\text{m}$ . (b) Simultaneous measurement of signals  $S_{FE}$  and  $S_Y$  versus time.

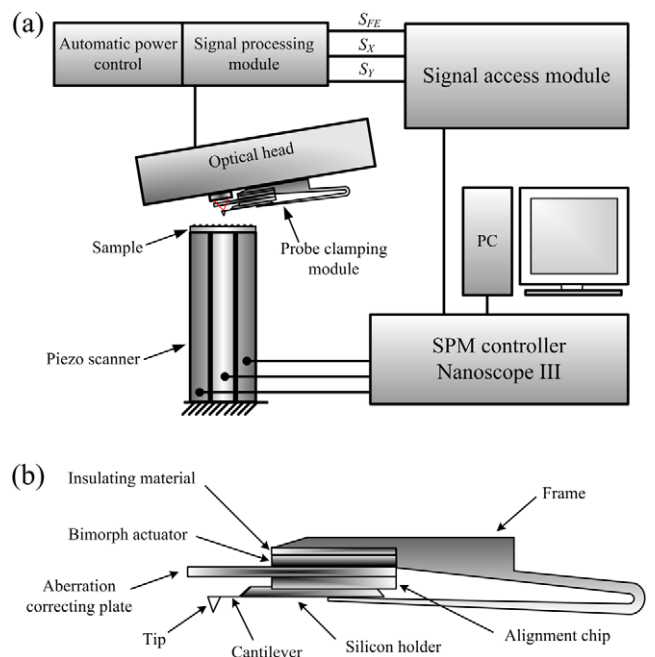


**Figure 6.** (a) Schematic drawing of a modified commercial AFM. (b) The probe clamping module contains a metal frame, an insulating material, a bimorph actuator, an aberration correcting plate and an alignment chip.

Figures 7(a) and (b) show tapping mode topographic images of a graphite surface taken with this modified AFM using the  $S_{FE}$  and  $S_Y$  signals to detect the bending motion of a cantilever, respectively. Single atomic steps can be clearly seen in both images. The height profiles show well-resolved single atomic steps of 0.32 nm. The surface roughness on

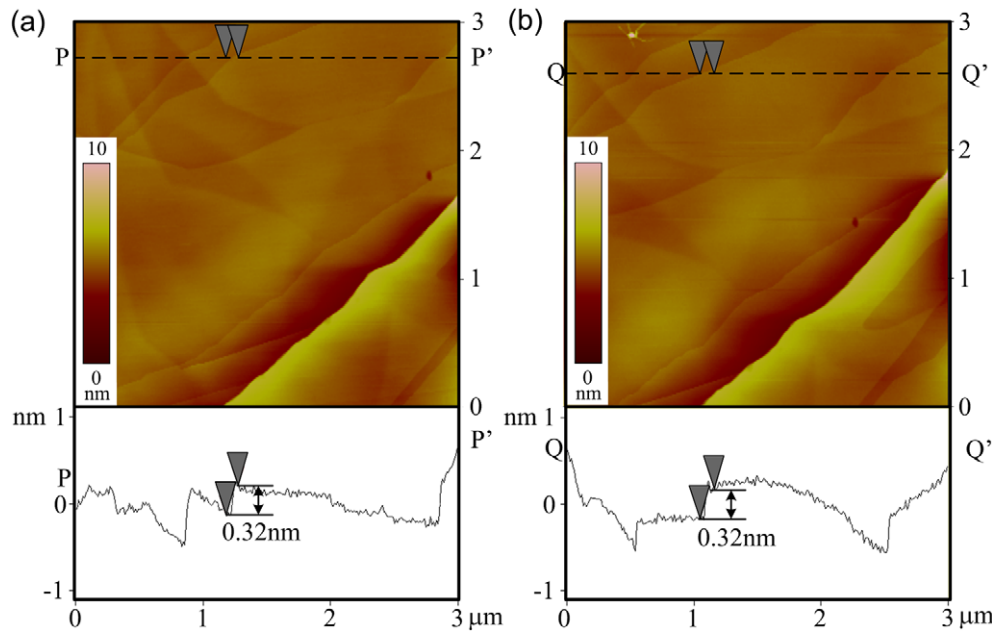


**Figure 7.** (a) Topographic image taken using the  $S_{FE}$  signal to detect the bending motion of an AFM cantilever. A height profile along the  $PP'$  line is shown at the bottom. (b) Topographic image taken using the  $S_Y$  signal to detect the bending motion of an AFM cantilever. A height profile along the  $QQ'$  line is shown at the bottom. The working frequency of the cantilever is 293.84 kHz.

flat graphite terraces is determined to be slightly smaller than 0.04 nm. This is as good as that obtained using the beam deflection module. Evidently, the  $S_{FE}$  and  $S_Y$  signals of our astigmatic detection system can provide good sensitivity in detection of the vertical displacement and angular deformation of the cantilever, respectively.

### 3.4. Measurement of thermal noise spectra of microfabricated cantilevers

We find that the  $S_{FE}$ ,  $S_Y$ , and  $S_X$  signals are sensitive enough to detect the small thermal motions of AFM cantilevers. Figure 8 shows the thermal noise spectra of an AFM cantilever, as measured with the  $S_{FE}$  and  $S_Y$  signals. Figure 8(a) shows the spectra taken near the free end of a cantilever. The peaks corresponding to thermal vibrations of the first and the second bending modes can be detected with both signals. As shown in figure 8(b), when the laser spot is focused at the node of the second bending mode, the peak corresponding to this mode disappears in the  $S_{FE}$  signal but remains visible in  $S_Y$ . The spectra also show that the noise level between 1 and 800 kHz is  $\sim 1.3 \text{ pm Hz}^{-1/2}$  for  $S_{FE}$  and  $\sim 3.2 \text{ nrad Hz}^{-1/2}$  for  $S_Y$ . These values are equivalent to or slightly higher than those for the laser interferometry (10–100 fm  $\text{Hz}^{-1/2}$ ) and for the beam deflection method used in commercial AFMs (0.5–5 nrad  $\text{Hz}^{-1/2}$ ).

In the measurement shown in figure 8(a), the laser beam is also focused on the main axis and near the free end of the cantilever, as illustrated in the inset of figure 9(a). Figure 9(a) shows the thermal noise spectra of the cantilever measured with the  $S_X$  signals. For comparison, the spectra taken with the  $S_{FE}$  signal is also shown, which is the same as that in figure 8(a). Note that the peaks corresponding to thermal vibrations of the

first and second torsional modes can be clearly detected with the  $S_X$  signal, but not with the  $S_{FE}$  signal. This is because the torsional modes involve only angular changes with no height variation on the main axis of the cantilever. When we move the focused laser spot away from the main axis, the  $S_{FE}$  signal can also detect the peak corresponding to the first torsional mode, as shown in figure 9(b).

One unexpected thing in figure 9 is that the fundamental bending mode is also detected with  $S_X$ . The first possibility is that there is a small misalignment for the orientation of our detection system relative to the long axis of the cantilever. Thus a small angular component around the  $Y$  axis is detected. The second possibility is that there is a coupling to the  $S_X$  signal from the vertical displacement. We believe that the first possibility can be ruled out because no torsional modes are detected with the  $S_Y$  signal in figures 8(a). This coupling can also explain the larger peaks corresponding to the torsional resonances detected with the  $S_X$  signal in figure 9(b) than the peaks in figure 9(a). The cause of the crosstalk will be further discussed in section 3.5.

We note that the higher noise levels for the spectra taken at frequencies  $\leq 1$  kHz are mainly caused by the mechanical stages used to adjust the position and the angular alignment of our detection system. To improve the low-frequency noise levels, one can try to enhance the rigidity of the system, as we have demonstrated in the modified AFM in figure 6. The electronic cutoff frequency of our detection system is  $\sim 800$  kHz, which is limited by the operational amplifiers we are using to generate the  $S_{FE}$ ,  $S_X$  and  $S_Y$  signals. It can be further improved if high-speed electronic components are adopted. As to the noise levels of our astigmatic detection system, they are mainly limited by the electronic circuits for driving the laser diode and for the signal processing.

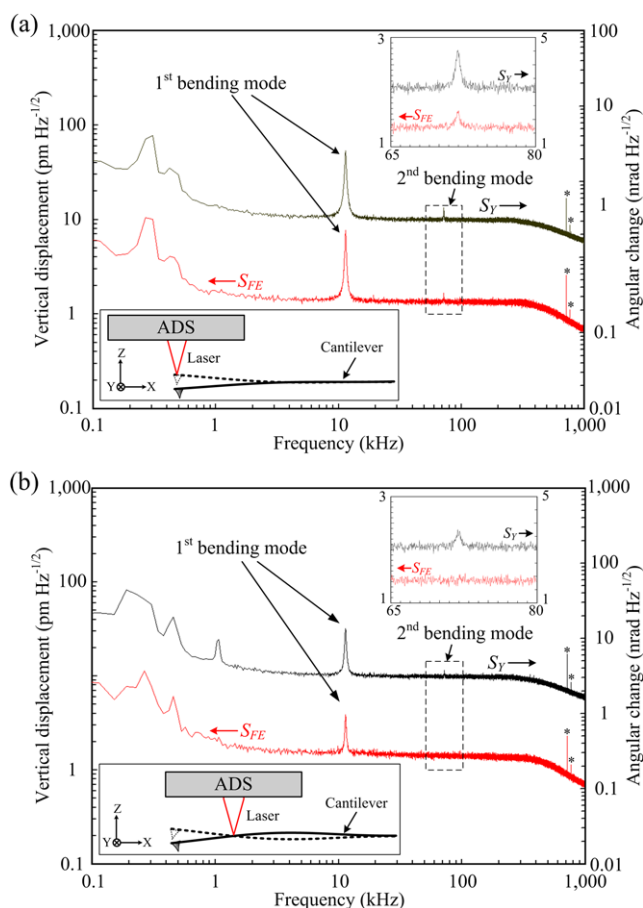


**Figure 8.** Thermal noise spectra of an AFM cantilever measured with the  $S_{FE}$  and  $S_Y$  signals. (a) Spectra measured near the free end of a cantilever. (b) Spectra measured at the node of the second bending mode of the cantilever. A schematic drawing of the measurement is shown at the lower left inset. A blow-up of the spectra near the second bending mode is shown at the upper right inset. The peaks marked with \* are caused by interferences of our electronic systems, rather than by mechanical resonances of the cantilever.

It has recently been shown that modulation of the laser power with a high-frequency signal can effectively reduce the ‘optical feedback noise’ and ‘optical interference noise’ by one to two orders of magnitude [23]. Thus, the noise levels of our detection system can be further improved through improvement in electronic circuits.

### 3.5. Advantages and drawbacks using DVD optical heads

We have demonstrated the measurements of vertical and angular displacements on micromachined cantilevers with the modified DVD optical heads. The success in getting good AFM images using this astigmatic detection system indicates that the system is sensitive enough for most applications, including the MEMS/NEMS-based chemical and biological sensors. It can also be applied to detect motions of a macro-object as long as it has a region of reflective surface with low roughness or is attached with a flat mirror, as we have demonstrated in the measurements shown in figure 3.

One important advantage for using the DVD optical head is that it can be operated over a wide frequency range.

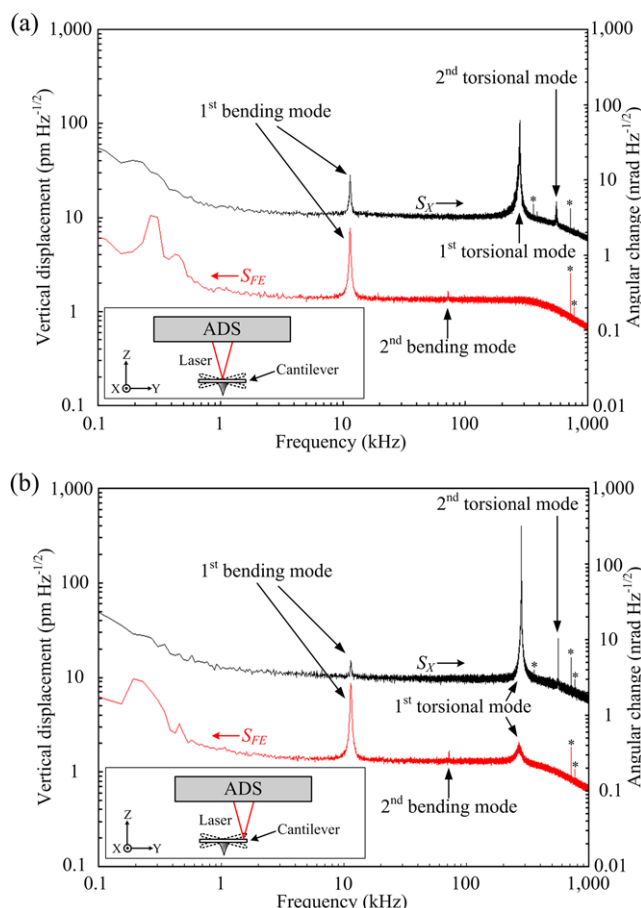


**Figure 9.** Thermal noise spectra taken at the free end of an AFM cantilever, as measured with the  $S_{FE}$  and  $S_X$  signals. (a) Measurements of the spectra with the focus spot on the main axis. (b) Measurements of the spectra with the focus spot on a side of the cantilever. A schematic drawing of the measurement is shown at the lower left inset.

Typical commercial DVD optical heads can detect signals at a rate over 60 MHz, and some systems can even reach beyond 260 MHz [24]. Operation at high frequencies is very desirable, because it can increase the response speed of AFM and improve the sensitivity of the MEMS/NEMS-based chemical and biological sensors. It may also be useful for other applications, such as detection of surface acoustic waves [25, 26]. Another advantage is that the focused spot size of DVD optical heads is only  $0.64 \mu\text{m}$ ; thus the laser beam can be easily focused at any desired location of micron-sized elements to carry out dynamic measurements.

In addition, DVD optical heads are small, compact, reliable and of very low cost. For the application in AFMs, the commercial DVD optical head weighs  $\sim 10$  g or less and costs  $\sim \$20$ ; the typical beam deflection module weighs several hundred grams and costs  $\sim \$10000$ . The light weight of the DVD optical head is especially favorable for the design of a stationary-sample type AFM [27]. The beam deflection module used in commercial AFMs is usually bulky and heavy, so the module and the cantilever are stationary and the sample is scanned with a piezo-scanner during the image taking. For a large and heavy sample, e.g. 12-inch silicon wafer, it is better

that the sample is kept stationary with the AFM cantilever scanned with a piezo-scanner. However, a sophisticated optical design is needed in order to track the motion of the cantilever in the 3D space [27]. Now the weight of the entire DVD optical head and the cantilever is so small that they can be driven directly by a piezo-scanner. This would greatly simplify the design of stationary-sample type AFMs.

It would be very desirable if the astigmatic detection system could be used to make quantitative measurements of the height and 2D tilt angles of an object surface over certain height and angular ranges. This will open many important applications in science and engineering. However, the height and the angular signals of our detection system are coupled to each other to a certain degree, depending on the dc values of height and tilt angles. This is because commercial DVD optical heads were originally designed for reading digital signals from optical disks, rather than for precision measurements. An example is the use of a low cost tilted glass plate [16] as the astigmatic lens in the DVD optical heads we are using, which introduces extra optical aberration. Furthermore, some edges of the projected light spot fall outside the photosensor, especially when there is a large non-zero tilt angle or defocus distance. We believe that the couplings can be significantly reduced if the optical components of the astigmatic system can be optimized for the precision measurements described above. Optical simulations, which will be presented elsewhere, have basically confirmed our observation of the shape change and the translation of the light spot on the quadrant photosensors caused by the changes in height and tilt angles, respectively. They also show much less crosstalk between the height and angular signals if a cylindrical lens is used as the astigmatic lens. In addition, the 6–8  $\mu\text{m}$  linear region for the  $S_{FE}$  signal in DVD optical heads may be too small for many applications. One can choose an objective lens with a smaller numerical aperture (NA) to increase the linear region.

The success of our astigmatic detection system suggests other detection schemes adopted in optical disk technologies might also provide high sensitivity in the detection of the vertical displacement and change in the tilt angle at a local position on an object surface. The focusing control is essential for any optical disk drive. Many techniques have been proposed for the derivation of the focus error signal [28–30]. These focus error signals also exhibit a similar S-curve as shown in figure 1 and can be used to detect the vertical displacement. We believe, through appropriate processing of signals from the photosensors, these optical detection techniques might also detect one- or two-dimensional angular tilt of an object surface.

#### 4. Conclusions

Here we have demonstrated an astigmatic detection system that can be used to characterize the static and dynamic mechanical responses of AFM cantilevers with a high sensitivity and over a wide frequency range. This detection scheme also

possesses several remarkable features, such as high sensitivity, dynamic measurements over a wide frequency range and a small detecting spot size. With further optimization of the optical components in our astigmatic detection system, this detection system may open new applications in many technological fields.

#### Acknowledgments

This research is supported by the National Science Council of ROC (contract nos. NSC95-2120-M-001-007 and NSC95-3114-P-001-008–MY3) and Academia Sinica.

#### References

- [1] Binnig G, Quate C F and Gerber Ch 1986 *Phys. Rev. Lett.* **56** 930
- [2] Wiesendanger R 1994 *Scanning Probe Microscopy and Spectroscopy* (Cambridge: Cambridge University Press)
- [3] Fritz J et al 2000 *Science* **288** 316
- [4] Lavrik N V, Sepaniak M J and Datskos P G 2004 *Rev. Sci. Instrum.* **75** 2229
- [5] Ilic B et al 2000 *Appl. Phys. Lett.* **77** 450
- [6] Li M, Tang H X and Roukes M L 2007 *Nat. Nanotechnol.* **2** 114
- [7] Burg T P et al 2007 *Nature* **446** 1066
- [8] den Boef A J 1989 *Appl. Phys. Lett.* **55** 439
- [9] Hoogenboom B H et al 2005 *Appl. Phys. Lett.* **86** 074101
- [10] Göddenhenrich T, Lemke H, Hartmann U and Heiden C 1990 *J. Vac. Sci. Technol. A* **8** 383
- [11] Meyer G and Amer N M 1988 *Appl. Phys. Lett.* **53** 1045
- [12] Compann K and Kramer P 1973 *Philips Tech. Rev.* **33** 178
- [13] Bouwhuis G and Braat J J M 1978 *Appl. Opt.* **17** 1993
- [14] Cohen D K, Gee W H, Ludeke M and Lewkowicz J 1984 *Appl. Opt.* **23** 565
- [15] Masud M 1987 *Appl. Opt.* **26** 3981
- [16] Zhang J and Cai L 1996 *IEEE. Instrumentation and Measurement Technology Conf. (Belgium, June)* p 513
- [17] Fan K C, Lin C Y and Shyu L H 2000 *Meas. Sci. Technol.* **11** N1
- [18] Quercioli F, Tiribilli B, Ascoli C, Baschieri P and Frediani C 1999 *Rev. Sci. Instrum.* **70** 3620
- [19] Hu E T, Huang K Y and Hwang I S 2004 *Proc. Optics East USA* vol 5602, p 218
- [20] Cooper E B et al 2000 *Appl. Phys. Lett.* **76** 3316
- [21] Taguchi A, Miyoshi T, Takaya Y and Takahashi S 2004 *Precis. Eng.* **28** 152
- [22] Hwu E T, Huang K Y, Hung S K and Hwang I S 2005 *Japan. J. Appl. Phys.* **45** 2368
- [23] Fukuma T et al 2005 *Rev. Sci. Instrum.* **76** 053704
- [24] Sturm J et al 2005 *IEEE J. Solid-State Circuits* **40** 1406
- [25] Deger C et al 1998 *Appl. Phys. Lett.* **72** 2400
- [26] Knuutila J V, Tikka P T and Salomaa M M 2000 *Opt. Lett.* **25** 613
- [27] Hung S K, Hwang I S and Fu L C 2004 *Proc. IMTC Italy* vol 3, p 1985
- [28] Kohno T, Ozawa N, Miyamoto K and Musha T 1988 *Appl. Opt.* **27** 103
- [29] Ehrmann K, Ho A and Schindheim K 1998 *Meas. Sci. Technol.* **9** 1259
- [30] Chu C L and Lin C H 2005 *Meas. Sci. Technol.* **16** 2498